WALAILAK JOURNAL
http://wjst.wu.ac.th Applied Mathematics

Radiation and Dufour Effects on Unsteady MHD Mixed Convective Flow in an Accelerated Vertical Wavy Plate with Varying Temperature and Mass Diffusion

Jagdish PRAKASH[1,*], Bangalore Rushi KUMAR[2] and Ramachandran SIVARAJ[2]

[1]*Department of Mathematics, University of Botswana, Gaborone, Botswana*
[2]*Fluid Dynamics Division, School of Advanced Sciences, VIT University, Vellore, India*

([*]Corresponding author's e-mail: prakashj@mopipi.ub.bw)

Received: 28 February 2013, Revised: 12 September 2013, Accepted: 13 October 2013

Abstract

This paper studies flow, heat, and mass transfer characteristics of unsteady mixed convective magnetohydrodynamic (MHD) flow of a heat absorbing fluid in an accelerated vertical wavy plate, subject to varying temperature and mass diffusion, with the influence of buoyancy, thermal radiation and Dufour effect. The momentum, energy and mass diffusion equations are coupled non-linear partial differential equations, which are solved by perturbation technique. The features of the fluid flow, heat and mass transfer characteristics are analyzed by plotting graphs, and the physical aspects are discussed in detail to interpret the effects of significant parameters of the problem.

Keywords: Radiation, Dufour effect, wavy plate, varying temperature, varying mass diffusion

Nomenclature

x	dimensional distances along the plate
y	dimensional distances perpendicular to the plate
u	component of dimensional velocity u along x directions
v	component of dimensional velocity u along y directions
g	gravitational acceleration
p	pressure
K^*	dimensional porosity parameter
B_0	magnetic field coefficient
T	dimensional temperature of the fluid
T_w	wall temperature
T_∞	ambient temperature
C_p	specific heat of constant pressure
k	thermal conductivity
Q	dimensional heat absorption coefficient
C_s	concentration susceptibility
K_T	thermal diffusion ratio

C dimensional concentration
C_w wall concentration
C_∞ ambient concentration
D molecular diffusivity
K_R dimensional chemical reaction parameter
u_p moving velocity of the plate
n^* dimensional positive real constant
t^* dimensional time
A real positive constant
V_0 scale of suction velocity
a^* amplitude of the wavy wall
Nu^* dimensional Nusselt number
Sh^* dimensional Sherwood number
B pressure gradient
G_r thermal Grashof number
G_c solutal Grashof number
M magnetic field parameter
K porosity parameter
P_r Prandtl number
F thermal radiation parameter
D_u Dufour number
S_c Schmidt number
K_r chemical reaction parameter
U_P moving velocity of the plate

Greek symbols

ρ density
μ dynamic viscosity
ν kinematic viscosity
σ magnetic permeability of the fluid
β_T thermal expansion coefficient
β_C concentration expansion coefficient
$\in$ small positive constant less than unity
τ^* dimensional skin friction coefficient
α_T heat absorption parameter

Introduction

Magnetohydrodynamic (MHD) heat transfer has gained significance owing to recent advancements in space technology. In recent years, considerable progress has been made in the study of heat and mass transfer with MHD flows due to its application in many devices, such as the MHD power generator and the Hall accelerator. We can realize the influence of magnetic fields from the works of Barletta *et al*. [1], Afify [2], Srinivas and Muthuraj [3], and Sivaraj and Rushi Kumar [4]. Mixed convection arises in many natural and technological processes; depending on the forced flow direction, the buoyancy forces may aid or oppose the forced flow, causing an increase or decrease in the heat transfer rates. The problem of mixed convection resulting from flow over a heated vertical plate is of considerable theoretical and practical interest. Mixed convection problems with different configurations are investigated by Yih [5], Barletle [6], Motsa [7] and Ching *et al*. [8]. The hot walls and the working fluid usually emit thermal radiation within the systems. The role of thermal radiation is of major importance in the design of many advanced energy convection systems operating at high temperatures, and knowledge of radiative heat transfer becomes very important in nuclear power plants, gas turbines and the various propulsion devices for aircraft, missiles and space vehicles. Murthy *et al*. [9], Grosan and Pop [10], Khaefinejad and Aghanajafi [11], and Prakash *et al*. [12] have made investigations of fluid flow with thermal radiation. Joule heating is a developing technology with considerable potential for the food industry. Convective flow with simultaneous heat and mass transfer under the influence of a magnetic field and chemical reaction have attracted considerable attention from researchers because such processes exist in many branches of science and technology. Chemical reactions can be codified as either heterogeneous or homogeneous processes. This depends on whether they occur at an interface or as a single phase volume reaction. The first order chemical reaction is one of the simplest chemical reactions, in which the rate of reaction is directly proportional to the species concentration. The present trend in the field of chemical reaction analysis is to give a mathematical model for the system to predict the reactor performance. The study of chemical reaction is useful in chemical processing industries, such as fiber drawing, crystal pulling from the melt, and polymer production. The engineering applications include chemical distillatory processes, formation and dispersion of fog, design of heat exchangers, channel type solar energy collectors, and thermo-protection systems. In view of these applications, Sivaraj and Kumar [13], Kandasamy *et al*. [14], Mansour *et al*. [15], Sivaraj and Kumar [16], and Kumar and Sivaraj [17] have examined the effect of chemical reaction.

When the heat and mass transfer occur simultaneously in a moving fluid, the relation between the fluxes and the driving potentials are more intricate in nature. The energy fluxes can also create concentration gradients, and this is the diffusion-thermo, or Dufour, effect. The Dufour effect is neglected on the basis that it is less significant than the effects described by Fourier and Fick's laws, because this effect is considered to be a second order phenomena. However, this effect is significant in areas such as hydrology, petrology and geo-sciences. We can realize the significance of the Dufour effect from the works of Anghel *et al*. [18], Postelnicu [19], Pal and Mondal [20], and Rushi Kumar and Sivaraj [21]. Previous studies of the flows of heat and mass transfer have focused mainly on a flat wall or a regular channel. It is necessary to study the heat and mass transfer in wavy plates because of its numerous applications. Fluid flow over wavy boundaries may be observed in several natural phenomena, viz., the generation of wind waves on water, the formation of sedimentary ripples in river channels, and dunes in the desert. The analysis of such flows finds applications in different areas, such as transpiration cooling of reentry vehicles and rocket boosters, cross-hatching on ablative surfaces, and film vaporization in combustion chambers. In view of these applications Jang *et al*. [22], Jang and Yan [23], and Mahdy *et al*. [24] had analyzed the fluid flow in wavy plates.

Motivated by the above referenced works and the numerous possible industrial applications of engineering fields, it is of paramount interest in this study to analyze the effect of unsteady mixed convective flow of a heat absorbing fluid in an accelerated vertical wavy plate, subject to varying temperature and mass diffusion. The main objective of this study is to examine the flow, heat and mass transfer characteristics of the significant physical parameters, such as thermal radiation parameter, Dufour number, and chemical reaction parameter in this problem.

Formulation of the problem

We consider unsteady two-dimensional flow of an incompressible, viscous, electrically conducting and heat-absorbing fluid past a semi-infinite vertical permeable wavy plate subject to varying temperature and concentration. A uniform transverse magnetic field of magnitude B_0 is applied in the presence of buoyancy effect in the direction of $y-$axis. The thermal radiation and diffusion thermo effects are present in the energy equation. The mass diffusion equation includes the first order chemical reaction. Other properties of the fluid are assumed to be constant.

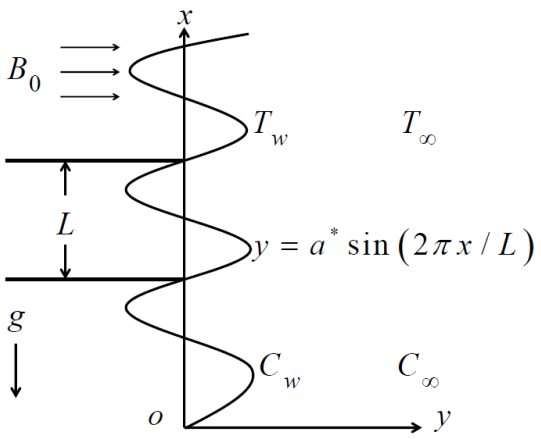

Figure 1 Schematic diagram of the problem.

The governing equations for this investigation are based on the balances of mass, linear momentum, energy and concentration species. Taking into consideration these assumptions, the equations that describe the physical situation can be written in a Cartesian frame of references, as follows;

$$\frac{\partial u}{\partial x}+\frac{\partial v}{\partial y}=0 \tag{1}$$

$$\frac{\partial u}{\partial t^*}+\left(u\frac{\partial u}{\partial x}+v\frac{\partial u}{\partial y}\right)=-\frac{1}{\rho}\frac{\partial p}{\partial x}+\nu\left(\frac{\partial^2 u}{\partial x^2}+\frac{\partial^2 u}{\partial y^2}\right)-\frac{\sigma B_0^2}{\rho}u-\frac{\nu}{K^*}u + g\beta_T\left(T-T_\infty\right)+g\beta_C\left(C-C_\infty\right) \tag{2}$$

$$\frac{\partial T}{\partial t^*}+\left(u\frac{\partial T}{\partial x}+v\frac{\partial T}{\partial y}\right)=\frac{k}{\rho C_p}\left(\frac{\partial^2 T}{\partial x^2}+\frac{\partial^2 T}{\partial y^2}\right)-\frac{Q\left(T-T_\infty\right)}{\rho C_p} -\frac{1}{\rho c_p}\left(\frac{\partial q}{\partial x}+\frac{\partial q}{\partial y}\right)+\frac{DK_T}{C_S C_p}\left(\frac{\partial^2 C}{\partial x^2}+\frac{\partial^2 C}{\partial y^2}\right) \tag{3}$$

$$\frac{\partial C}{\partial t^*}+\left(u\frac{\partial C}{\partial x}+v\frac{\partial C}{\partial y}\right)=D\left(\frac{\partial^2 C}{\partial x^2}+\frac{\partial^2 C}{\partial y^2}\right)-K_R\left(C-C_\infty\right) \tag{4}$$

The boundary conditions of the problem are;

$$t^*\le 0: \quad u=0, \quad T=T_\infty, \quad C=C_\infty \quad for\ all \quad y \tag{5}$$

$$t^*>0: \quad u=u_P, \quad \frac{\partial T}{\partial y}=A_1T_w, \quad \frac{\partial C}{\partial y}=A_1C_w \quad at \quad y=a^*\sin\left(2\pi x/L\right) \tag{6}$$

$$u\to u_\infty=u_0\left(1+\in e^{n^*t^*}\right), \quad T_w\to T_\infty, \quad C_w\to C_\infty \quad as \quad y\to\infty \tag{7}$$

Since the motion is two dimensional and the length of the plate is large enough, all the physical variables are independent of the $x-$ coordinate. Therefore;

$$\frac{\partial u}{\partial x}=0 \tag{8}$$

so that the suction velocity at the plate surface is a function of time only, and we assume that the suction velocity takes the following exponential form;

$$v=-V_0\left(1+\in Ae^{n^*t^*}\right) \tag{9}$$

where A is a real positive constant, $\in$ and $\in A$ are less than unity, and V_0 is a scale of suction velocity which has a non-zero positive constant.

Outside the boundary layer, Eq. (2) gives;

$$-\frac{1}{\rho}\frac{dp}{dx}=\frac{du_\infty}{dt^*}+\left(\frac{\sigma B_0^2}{\rho}+\frac{K^*}{\mu}\right)u_\infty=B \tag{10}$$

so that the pressure p is independent of y.

The fluid is optically thin, with a relatively low density, and the radiative heat flux discussed by Cogley *et al*. [25] is given by;

$$\frac{\partial q}{\partial Y}=4\left(T_0-T\right)I' \tag{11}$$

where $I'=\int_0^\infty K_{\lambda w}\frac{\partial e_{b\lambda}}{\partial T}d\lambda$, $K_{\lambda w}$ is the radiation absorption coefficient at the wall and $e_{b\lambda}$ is Plank's function.

Introducing the following non-dimensional quantities;

$$U=\frac{u}{U_0},\ V=\frac{v}{V_0},\ X=\frac{x}{L},\ Y=\frac{V_0 y}{\nu},\ U_\infty=\frac{u_\infty}{U_0},\ t=\frac{V_0^2 t^*}{\nu},\ \theta=\frac{T-T_\infty}{T_w-T_\infty},\ \phi=\frac{C-C_\infty}{C_w-C_\infty},$$

$$n=\frac{n^*\nu}{V_0^2},\quad M=\frac{\sigma B_0^2\nu}{\rho V_0^2},\ K=\frac{\nu^2}{V_0^2K^*},\ N=\left(M+\frac{1}{K}\right),\ G_r=\frac{\nu g\beta_T\left(T_w-T_\infty\right)}{U_0V_0^2},$$

$$G_c=\frac{\nu g\beta_C\left(C_w-C_\infty\right)}{U_0V_0^2},\ P_r=\frac{\mu C_p}{k},\ \alpha_T=\frac{Q\nu}{\rho C_pV_0^2},\ F=\frac{4I'}{\rho C_pV_0},\ S_c=\frac{\nu}{D},$$

$$D_u=\frac{DK_T\left(C_w-C_\infty\right)}{\nu C_sC_pV_0^2\left(T_w-T_\infty\right)},\ K_r=\frac{K_R\nu}{V_0^2},\ U_P=\frac{u_p}{U_0},\ A_1=\frac{V_0}{\nu},\ h=a\sin\left(2\pi X\right) \tag{12}$$

The basic Eqs. (2) to (4) can be expressed in non-dimensional form as;

$$\frac{\partial U}{\partial t}-\left(1+\in Ae^{nt}\right)\frac{\partial U}{\partial Y}=\frac{\partial^2U}{\partial Y^2}-NU+G_r\theta+G_c\phi+B=0 \tag{13}$$

$$\frac{\partial\theta}{\partial t}-\left(1+\in Ae^{nt}\right)\frac{\partial\theta}{\partial Y}=\frac{1}{P_r}\frac{\partial^2\theta}{\partial Y^2}-\left(F+\alpha_T\right)\theta+D_u\frac{\partial^2\phi}{\partial Y^2}=0 \tag{14}$$

$$\frac{\partial\phi}{\partial t}-\left(1+\in Ae^{nt}\right)\frac{\partial\phi}{\partial Y}=\frac{1}{S_c}\frac{\partial^2\phi}{\partial Y^2}-K_r\phi \tag{15}$$

The boundary conditions become;

$$t\le 0:\quad U=0,\quad \theta=0,\quad \phi=0\quad for\ \ all\quad Y \tag{16}$$

$$t>0:\quad U=U_P,\quad \frac{\partial\theta}{\partial y}=1,\quad \frac{\partial\phi}{\partial y}=1\quad at\quad Y=h \tag{17}$$

$$U\to U_\infty=1+\in e^{nt},\quad \theta\to 0,\quad \phi\to 0\quad as\quad Y\to\infty \tag{18}$$

Method of solution

The set of partial differential Eqs. (13) - (15) cannot be solved in closed-form. However, these equations can be solved analytically by using perturbation method after reducing them to a set of ordinary differential equations in dimensionless form. This can be done when the amplitude of oscillations $\in$ $\left(\in<<1\right)$ is very small. We can assume the solutions of flow velocity U, temperature θ and concentration ϕ in the neighborhood of the plate as;

$$U\left(Y,t\right)=U_0\left(Y\right)+\in e^{nt}U_1\left(Y\right)+o\left(\in^2\right) \tag{19}$$

$$\theta(Y,t) = \theta_0(Y) + \in e^{nt}\theta_1(Y) + o(\in^2) \tag{20}$$

$$\phi(Y,t) = \phi_0(Y) + \in e^{nt}\phi_1(Y) + o(\in^2) \tag{21}$$

On substituting the expressions in Eqs. (19) - (21) into Eqs. (13) - (15), equating harmonic and non-harmonic terms, and neglecting the higher-order terms of $o(\in^2)$, we get the following set of equations for U_0, θ_0, ϕ_0 and U_1, θ_1, ϕ_1.

$$U_0'' + U_0' - NU_0 = -(G_r\theta_0 + G_c\phi_0 + B) \tag{22}$$

$$U_1'' + U_1' - (N+n)U_1 = -(G_r\theta_1 + G_c\phi_1 + AU_0') \tag{23}$$

$$\theta_0'' + P_r\theta_0' - P_r(\alpha_T + F)\theta_0 = -D_u P_r\phi_0'' \tag{24}$$

$$\theta_1'' + P_r\theta_1' - P_r(\alpha_T + F + n)\theta_1 = -P_r(A\theta_0' + D_u\phi_0'') \tag{25}$$

$$\phi_0'' + S_c\phi_0' - S_cK_r\phi_0 = 0 \tag{26}$$

$$\phi_1'' + S_c\phi_1' - S_c(K_r + n)\phi_1 = -AS_c\phi_0' \tag{27}$$

where the prime denotes ordinary differentiation with respect to Y.

The corresponding boundary conditions are;

$$U_0 = U_P, \quad U_1 = 0, \quad \theta_0' = 1, \quad \theta_1' = 0, \quad \phi_0' = 1, \quad \phi_1' = 0 \qquad at \qquad Y = h \tag{28}$$

$$U_0 = 1, \quad U_1 = 1, \quad \theta_0 \to 0, \quad \theta_1 \to 0, \quad \phi_0 \to 0, \quad \phi_1 \to 0 \qquad as \qquad Y \to \infty \tag{29}$$

The solutions of Eqs. (22) - (27) subject to the boundary conditions (28) and (29) are as follows;

$$U_0 = A_{11}e^{-\beta_1 Y} + A_{12}e^{-\beta_3 Y} + A_{13} + A_{14}e^{-\beta_5 Y} \tag{30}$$

$$U_1 = A_{15}e^{-\beta_1 Y} + A_{16}e^{-\beta_2 Y} + A_{17}e^{-\beta_3 Y} + A_{18}e^{-\beta_4 Y} + A_{19}e^{-\beta_5 Y} + (A_{20} + A_{21})e^{-\beta_6 Y} \tag{31}$$

$$\theta_0 = A_4e^{-\beta_1 Y} + A_5e^{-\beta_3 Y} \tag{32}$$

$$\theta_1 = (A_6 + A_8)e^{-\beta_1 Y} + A_7e^{-\beta_2 Y} + A_9e^{-\beta_3 Y} + A_{10}e^{-\beta_4 Y} \tag{33}$$

$$\phi_0 = A_1 e^{-\beta_1 Y} \tag{34}$$

$$\phi_1 = A_2 e^{-\beta_1 Y} + A_3 e^{-\beta_2 Y} \tag{35}$$

On substituting the solutions in Eqs. (30) - (35) into Eqs. (19) - (21), we get the final form of velocity, temperature and concentration distributions in the boundary layer as follows;

$$\begin{aligned} U(Y,t) = &\left[A_{11} e^{-\beta_1 Y} + A_{12} e^{-\beta_3 Y} + A_{13} + A_{14} e^{-\beta_5 Y} \right] + \\ &\in e^{nt} \left[A_{15} e^{-\beta_1 Y} + A_{16} e^{-\beta_2 Y} + A_{17} e^{-\beta_3 Y} + A_{18} e^{-\beta_4 Y} + A_{19} e^{-\beta_5 Y} + \left(A_{20} + A_{21} \right) e^{-\beta_6 Y} \right] \end{aligned} \tag{36}$$

$$\begin{aligned} \theta(Y,t) = &\left[A_4 e^{-\beta_1 Y} + A_5 e^{-\beta_3 Y} \right] \\ &+ \in e^{nt} \left[\left(A_6 + A_8 \right) e^{-\beta_1 Y} + A_7 e^{-\beta_2 Y} + A_9 e^{-\beta_3 Y} + A_{10} e^{-\beta_4 Y} \right] \end{aligned} \tag{37}$$

$$\phi(Y,t) = \left[A_1 e^{-\beta_1 Y} \right] + \in e^{nt} \left[A_2 e^{-\beta_1 Y} + A_3 e^{-\beta_2 Y} \right] \tag{38}$$

The shear stress, the coefficient of the rate of heat transfer, and the rate of mass transfer at any point in the fluid can be characterized by;

$$\tau^* = -\mu \frac{\partial u}{\partial y};\ Nu^* = -k \frac{\partial T}{\partial y};\ Sh^* = -D \frac{\partial C}{\partial y} \tag{39}$$

In dimensionless form;

$$\tau = \frac{\tau^*}{\rho U_0 V_0} = -U';\ Nu = \left(\frac{Nu^* \nu}{k V_0 \left(T_w - T_\infty \right)} \right) = -\theta';\ Sh = \left(\frac{Sh^* \nu}{D V_0 \left(C_w - C_\infty \right)} \right) = -\phi' \tag{40}$$

The skin friction (τ), the Nusselt number (Nu) and the Sherwood number (Sh) at the wavy wall $Y = h$ are given by;

$$\begin{aligned} \tau = -U'\big|_{Y=h} = &\left[A_{11} \beta_1 e^{-\beta_1 h} + A_{12} \beta_3 e^{-\beta_3 h} + A_{14} \beta_5 e^{-\beta_5 h} \right] + \in e^{nt} \left[A_{15} \beta_1 e^{-\beta_1 h} + A_{16} \beta_2 e^{-\beta_2 h} + \right. \\ &\left. A_{17} \beta_3 e^{-\beta_3 h} + A_{18} \beta_4 e^{-\beta_4 h} + A_{19} \beta_5 e^{-\beta_5 h} + \left(A_{20} + A_{21} \right) \beta_6 e^{-\beta_6 h} \right] \end{aligned} \tag{41}$$

$$\begin{aligned} Nu = -\theta'\big|_{Y=h} = &\left[A_4 \beta_1 e^{-\beta_1 h} + A_5 \beta_3 e^{-\beta_3 h} \right] \\ &+ \in e^{nt} \left[\left(A_6 + A_8 \right) \beta_1 e^{-\beta_1 h} + A_7 \beta_2 e^{-\beta_2 h} + A_9 \beta_3 e^{-\beta_3 h} + A_{10} \beta_4 e^{-\beta_4 h} \right] \end{aligned} \tag{42}$$

$$Sh = -\phi'\big|_{Y=h} = \left[A_1 \beta_1 e^{-\beta_1 h} \right] + \in e^{nt} \left[A_2 \beta_1 e^{-\beta_1 h} + A_3 \beta_2 e^{-\beta_2 h} \right] \tag{43}$$

where the primes denote the derivative with respect to Y .

Results and discussion

In order to gain physical insight into this problem, the flow, heat and mass transfer profiles are discussed by assigning numerical values to various parameters obtained in the mathematical formulation of the problem, and the results graphically shown in **Figures 2 - 19**. Throughout the computations we employ $a = 0.5$, $n = 0.2$, $M = 1$, $t = 1$, $G_r = 4$, $G_c = 2$, $K = 2$, $P_r = 0.71$, $B = 0.5$, $S_c = 0.96$, $\alpha_T = 1$, $F = 1$, $D_u = 1$, $K_r = 1$, $\varepsilon = 0.02$, and $X = 1$, unless otherwise stated.

Figures 2 - 7 shows the effect of various significant parameters on the velocity distribution (U) with respect to Y. **Figure 2** illustrates the effect of magnetic field on the velocity distribution. The presence of transverse magnetic field produces a resistive force on the fluid flow. This force is called the Lorentz force, which slows down the motion of electrically conducting fluid. **Figure 3** is plotted to show the effect of porous permeability parameter. The increase in the porous permeability parameter accelerates the fluid velocity. **Figures 4** and **5** display the influence of the thermal Grashof number and solutal Grashof number respectively. As usual, increase in Grashof numbers considerably enhances the fluid flow. **Figure 6** illustrates the vital role of the chemical reaction parameter on the fluid velocity. The velocity of the fluid falls with increase in the chemical reaction parameter. **Figure 7** shows the influence of the velocity of the moving plate. It is observed that the velocity increases with increase velocity of the moving plate.

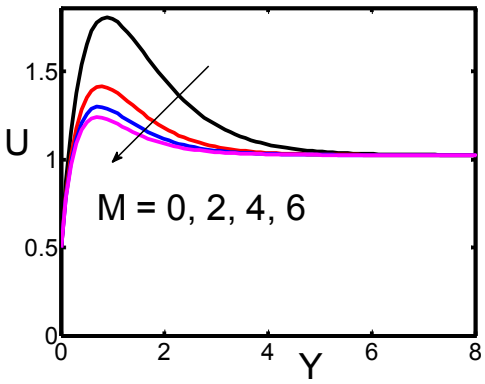

Figure 2 Effect of magnetic field parameter on velocity distribution.

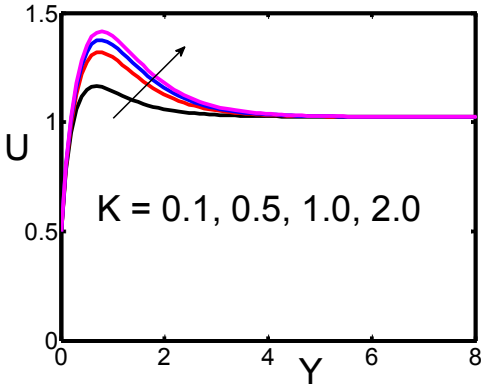

Figure 3 Effect of porous permeability parameter on velocity distribution.

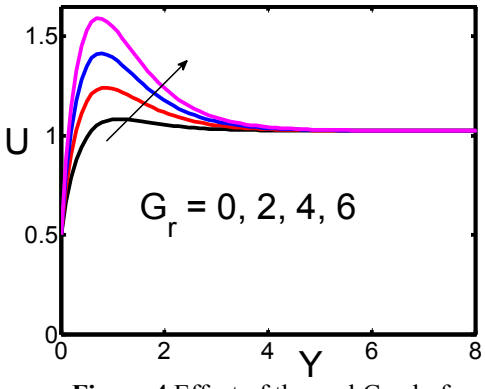

Figure 4 Effect of thermal Grashof number on velocity distribution.

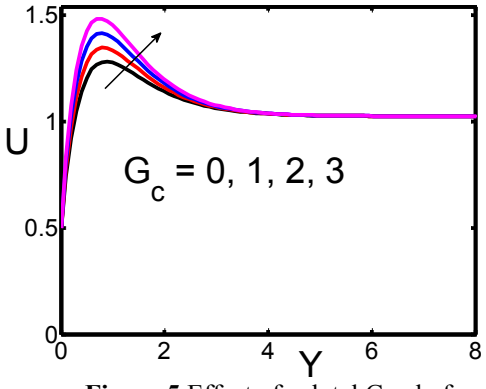

Figure 5 Effect of solutal Grashof number on velocity distribution.

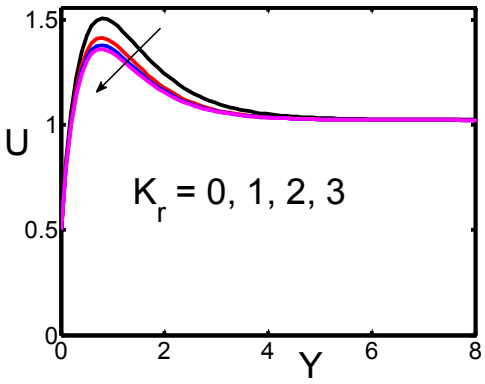

Figure 6 Effect of chemical reaction parameter on velocity distribution.

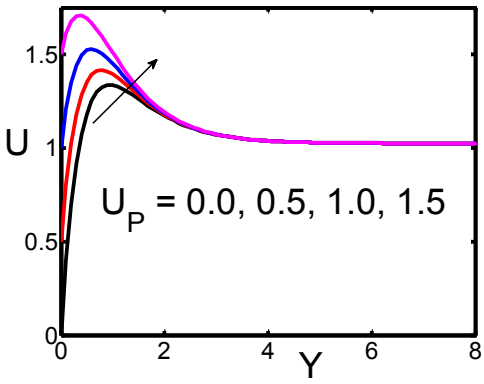

Figure 7 Effect of velocity of the moving plate on velocity distribution.

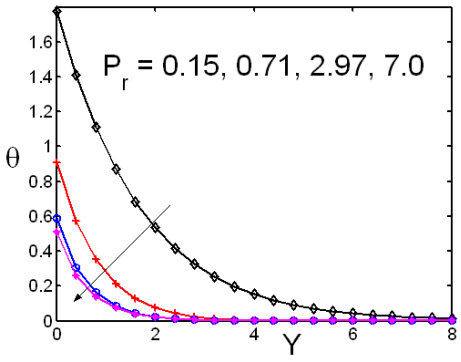

Figure 8 Effect of Prandtl number on temperature distribution.

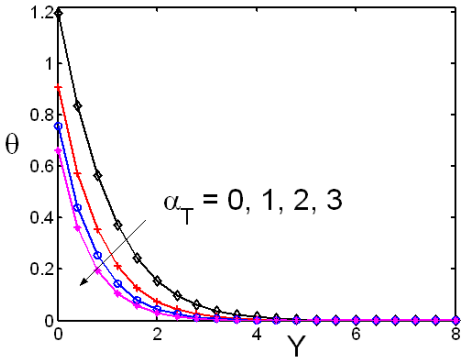

Figure 9 Effect of heat absorption parameter on temperature distribution.

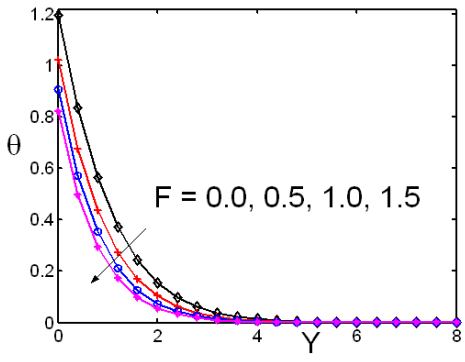

Figure 10 Effect of thermal radiation parameter on temperature distribution .

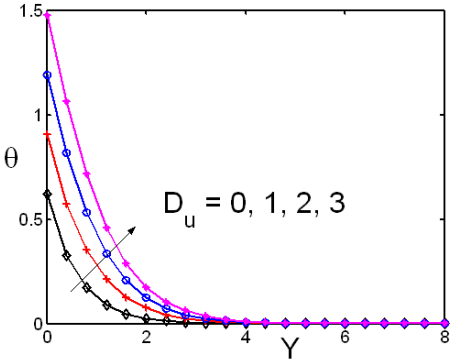

Figure 11 Effect of Dufour number on temperature distribution.

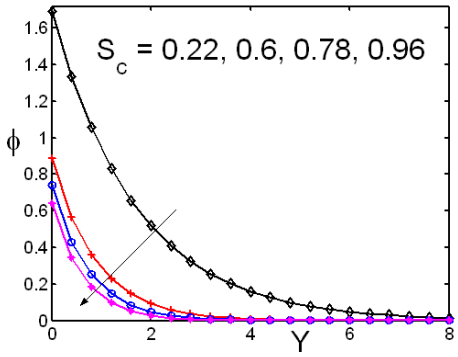

Figure 12 Effect of thermal radiation parameter on concentration distribution.

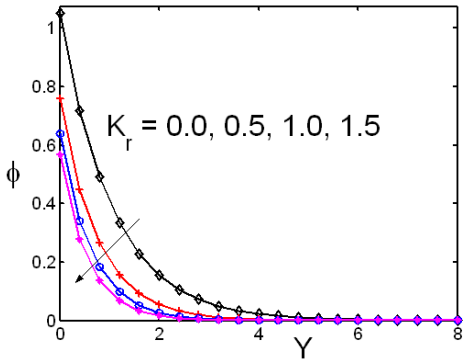

Figure 13 Effect of Dufour number on concentration distribution.

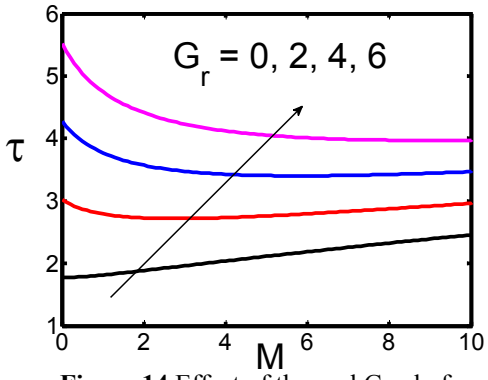

Figure 14 Effect of thermal Grashof number on skin friction distribution.

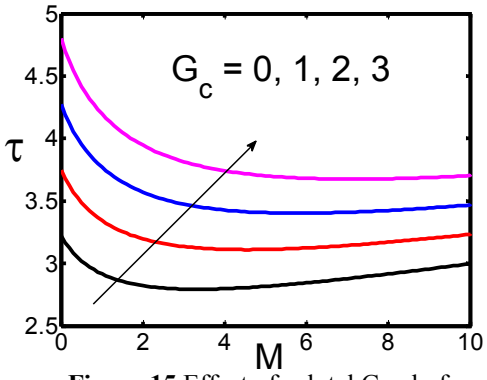

Figure 15 Effect of solutal Grashof number on skin friction distribution.

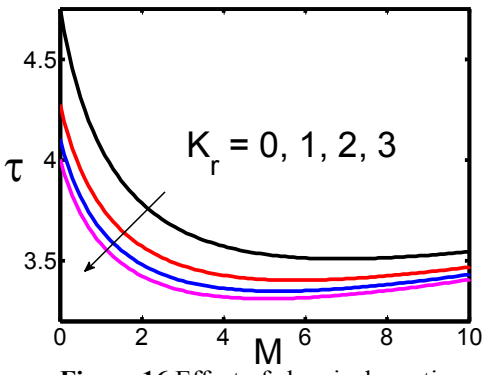

Figure 16 Effect of chemical reaction parameter on skin friction distribution.

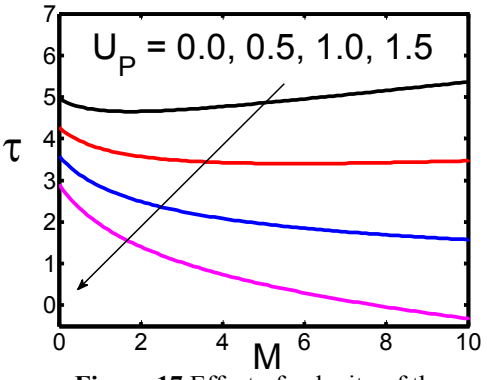

Figure 17 Effect of velocity of the moving plate on skin friction distribution.

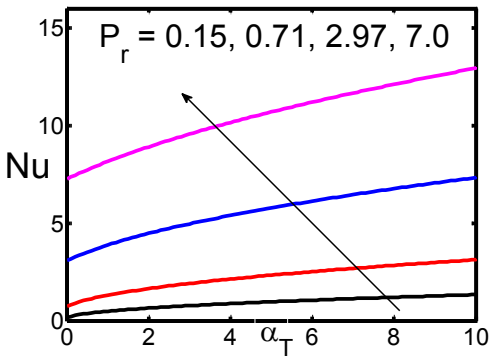

Figure 18 Effect of Prandtl number on Nusselt number distribution.

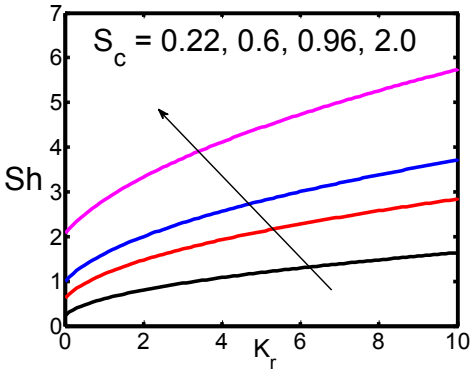

Figure 19 Effect of Schmidt number on Sherwood number distribution.

The temperature distribution against Y for different values of the parameters P_r, α_T, F and D_u are graphically displayed in **Figures 8 - 11**. It is observed from **Figure 8** that an increase in the Prandtl number results in a decrease of heat transfer profiles. This is because an increase in Prandtl number value is equivalent to an increase in the thermal conductivity and, therefore, heat is able to diffuse away from the heated cone and plate more rapidly. Hence, in the case of increasing Prandtl number, the boundary layer is thinner and the heat transfer is reduced. In the simulation, the values of Prandtl number used are 0.15, 0.71, 2.97 and 7.0; these correspond to noble gases with hydrogen, air, methyl chloride and water, respectively. **Figure 9** depicts the effect of heat sink parameter on temperature distribution. It is clear from the figure that the boundary layer absorbs the energy, resulting in the temperature falling for increasing values of heat absorption parameter. **Figure 10** shows that an increase in the radiation parameter decreases the temperature distribution, because large values of radiation parameter enhance the conduction over radiation, thereby decreasing the thickness of the thermal boundary layer. **Figure 11** shows that an increase in Dufour number significantly increases the thermal boundary layer thickness, which increases the fluid temperature.

Concentration distribution against Y for different values of the parameters S_c and K_r are shown in **Figures 12** and **13**. It is observed from **Figure 12** that an increase in Schmidt number decreases the mass transfer profiles. Physically, the increase in Schmidt number means a decrease of molecular diffusion. Hence, the mass transfer of the species is higher for small values of Schmidt number, and lower for larger values of Schmidt number. The values of the Schmidt number are chosen to represent the presence of species by hydrogen (0.22), water vapor (0.6), ammonia (0.78) and carbon dioxide (0.96). It is clear from **Figure 13** that we obtain a destructive type chemical reaction, because the concentration notably decreases when increasing the chemical reaction parameter, which indicates that the diffusion rates can be changed tremendously by the chemical reaction.

Figures 14 - 17 illustrate the effects of G_r, G_c, K_r and U_P on skin friction distribution (τ) against the magnetic field parameter. **Figures 14** and **15** show that an increase in thermal and solutal Grashof numbers increase the skin friction. It is observed from **Figures 16** and **17** that the skin friction diminishes when increasing the chemical reaction parameter and velocity of the moving plate. The significance of Prandtl number in the Nusselt number distribution (Nu) with respect to the heat absorption parameter (α_T) is shown in **Figure 18**. We observe that an increase in Prandtl number gradually increases the magnitude of Nusselt number. **Figure 19** is plotted to display the effect of Schmidt number on Sherwood number (Sh) with respect to the chemical reaction parameter (K_r). The Sherwood number strictly increases for the higher values of Schmidt number.

Conclusions

We have analyzed the flow, heat and mass transfer characteristics of unsteady mixed convective flow of a heat absorbing fluid in an accelerated vertical wavy plate, subject to varying temperature and mass diffusion. We noticed the following key observations from this study. Velocity decreases with an increase in magnetic field parameter, whereas it increases with an increase in porous permeability parameter, thermal Grashof number and solutal Grashof number. An increase in Prandtl number or heat sink parameter or thermal radiation parameter decreases the heat transfer, but the Dufour number reverses the trend. The fluid concentration decreases for increasing Schmidt number and chemical reaction parameter. The effects of various significant physical parameters on skin friction, Nusselt number and Sherwood number are illustrated graphically. Furthermore, it is clear from this study that the Dufour effect should be considered for fluids with light molecular weight.

Acknowledgements

The first author wishes to thank the Department of Science and Technology, New Delhi, India, for the prestigious "C. V. Raman International Fellowship for African Researchers-2011" award that enabled him to work with other co-authors at VIT University, Vellore, India, from 14 May 2012 - 14 August 2012. Further, the authors are thankful to the reviewers for their suggestions, which significantly improved their paper.

References

[1] A Barletta, S Lazzari, E Magyari and I Pop. Mixed convection with heating effects in a vertical porous annulus with a radially varying magnetic field. *Int. J. Heat Mass Tran*. 2008; **51**, 5777-84.
[2] A Afify. Similarity solution in MHD effects of thermal diffusion and diffusion thermo on free convective heat and mass transfer over a stretching surface considering suction or injection. *Comm. Nonlinear Sci. Numer. Simulat*. 2009; **14**, 2202-14.
[3] S Srinivas and R Muthuraj. Effects of thermal radiation and space porosity on MHD mixed convection flow in a vertical channel using homotopy analysis method. *Comm. Nonlinear Sci. Numer. Simulat*. 2010; **15**, 2098-108.
[4] R Sivaraj and BR Kumar. Viscoelastic fluid flow over a moving vertical cone and flat plate with variable electric conductivity. *Int. J. Heat Mass Tran.* 2013; **61**, 119-28.
[5] KA Yih. The effect of transpiration on coupled heat and mass transfer in mixed convection over a vertical plate embedded in a saturated porous medium. *Int. Comm. Heat Mass Tran*. 1997; **24**, 265-75.
[6] A Barletle. Combined forced and free convection with viscous dissipation in a vertical duct. *Int. J. Heat Mass Tran.* 1999; **42**, 2243-53.
[7] SS Motsa. The effects of thermal radiation, hall currents, Soret, and Dufour on MHD flow by mixed convection over a vertical surface in porous media. *SAMSA J. Pure Appl. Math*. 2008; **3**, 58-65.
[8] YC Ching, HF Oztop, MM Rahman, MR Islam and A Ahsan. Finite element simulation of mixed convection heat and mass transfer in a right triangular enclosure. *Int. Comm. Heat Mass Tran*. 2012; **39**, 689-96.
[9] PVSN Murthy, S Mukherjee, D Srinivasacharya and PVSSSR Krishna. Combined radiation and mixed convection from a vertical wall with suction/injection in a non-Darcy porous medium. *Acta Mechanica* 2004; **168**, 145-56.
[10] T Grosan and I Pop. Thermal radiation effect on fully developed mixed convection flow in a vertical channel. *Tech. Mech*. 2007; **1**, 37-47.
[11] B Khaefinejad and C Aghanajafi. Laminar flow with simultaneously effects of mixed convection and thermal radiation in a channel. *J. Fusion Energ*. 2009; **28**, 83-90.
[12] J Prakash, R Sivaraj and BR Kumar. Influence of chemical reaction on unsteady MHD mixed convective flow over a moving vertical porous plate. *Int. J. Fluid Mech*. 2011; **3**, 1-14.

[13] R Sivaraj and BR Kumar. Chemically reacting dusty viscoelastic fluid flow in an irregular channel with convective boundary. *Ain Shams Eng. J*. 2013; **4**, 93-101.
[14] R Kandasamy, K Periasamy and KKS Prabhu. Effects of chemical reaction, heat and mass transfer along a wedge with heat source and concentration in the presence of suction or injection. *Int. J. Heat Mass Tran*. 2005; **48**, 1388-94.
[15] MA Mansour, NF El-Anssary and AM Aly. Effects of chemical reaction and thermal stratification on MHD free convective heat and mass transfer over a vertical stretching surface embedded in a porous media considering Soret and Dufour numbers. *Chem. Eng. J.* 2008; **145**, 340-5.
[16] R Sivaraj and BR Kumar. Unsteady MHD dusty viscoelastic fluid Couette flow in an irregular channel with varying mass diffusion. *Int. J. Heat Mass Tran*. 2012; **55**, 3076-89.
[17] BR Kumar and R Sivaraj. Heat and mass transfer in MHD viscoelastic fluid flow over a vertical cone and flat plate with variable viscosity. *Int. J. Heat Mass Tran.* 2013; **56**, 370-9.
[18] M Anghel, HS Takhar and I Pop. Dufour and Soret effects on free-convection boundary layer over a vertical surface embedded in a porous medium. *Studia. Univ. Babes-Bolyai Math*. 2000; **45**, 11-21.
[19] A Postelnicu. Influence of chemical reaction on heat and mass transfer by natural convection from vertical surfaces in porous media considering Soret and Dufour effects. *Heat Mass Tran*. 2007; **43**, 595-602.
[20] D Pal and H Mondal. Soret and Dufour effects on MHD non-Darcian mixed convection heat and mass transfer over a stretching sheet with non-uniform heat source/sink. *Phys. B* 2012; **407**, 642-51.
[21] BR Kumar and R Sivaraj. MHD viscoelastic fluid non-Darcy flow over a vertical cone and a flat plate. *Int. Comm. Heat Mass Tran*. 2013; **40**, 1-6.
[22] JH Jang, WM Yan and HC Liu. Natural convection heat and mass transfer along a vertical wavy surface. *Int. J. Heat Mass Tran.* 2003; **46**, 1075-83.
[23] JH Jang and WM Yan. Mixed convection heat and mass transfer along a vertical wavy surface. *Int. J. Heat Mass Tran*. 2004; **47**, 419-28.
[24] A Mahdy, RA Mohamed and FM Hady. Heat and mass transfer in MHD free convection along a vertical wavy plate with variable surface heat and mass flux. *Lat. Am. Appl. Res.* 2009; **39**, 337-44.
[25] AC Cogley, WG Vincent and SE Giles. Differential approximation to radiative heat transfer in a non-grey gas near equilibrium. *Am. Inst. Aeronaut. Astronaut*. 1968; **6**, 551-3.

Appendix

$$\beta_1 = \frac{S_c + \sqrt{S_c{}^2 + 4S_c K_r}}{2},$$

$$\beta_2 = \frac{S_c + \sqrt{S_c^2 + 4S_c\left(K_r + n\right)}}{2},$$

$$\beta_3 = \frac{P_r + \sqrt{P_r^2 + 4P_r\left(\alpha_T + F\right)}}{2},$$

$$\beta_4 = \frac{P_r + \sqrt{P_r^2 + 4P_r\left(\alpha_T + F + n\right)}}{2},$$

$$\beta_5 = \frac{1 + \sqrt{1 + 4N}}{2},$$

$$\beta_6 = \frac{1 + \sqrt{1 + 4\left(N + n\right)}}{2},$$

$$A_1 = \frac{-e^{-\beta_1 h}}{\beta_1},$$

$$A_2 = \frac{AA_1\beta_1 S_c}{\beta_1^2 - Sc\left(\beta_1 + K_r + n\right)},$$

$$A_3 = \frac{-A_2\beta_1 e^{-\beta_1 h}}{\beta_2 e^{-\beta_2 h}},$$

$$A_4 = \frac{-A_1 P_r D_u \beta_1^2}{\beta_1^2 - P_r\left(\beta_1 + \alpha_T + F\right)},$$

$$A_5 = \frac{1 + A_4\beta_1 e^{-\beta_1 h}}{-\beta_3 e^{-\beta_3 h}},$$

$$A_6 = \frac{-A_2 P_r D_u \beta_1^2}{\beta_1^2 - P_r\left(\beta_1 + \alpha_T + F + n\right)},$$

$$A_7 = \frac{-A_3 P_r D_u \beta_2^2}{\beta_2^2 - P_r\left(\beta_2 + \alpha_T + F + n\right)},$$

$$A_8 = \frac{AA_4 P_r \beta_1}{\beta_1^2 - P_r\left(\beta_1 + \alpha_T + F + n\right)},$$

$$A_9 = \frac{AA_5 P_r \beta_3}{\beta_3^2 - P_r\left(\beta_3 + \alpha_T + F + n\right)},$$

$$A_{10} = \frac{1}{-\beta_4 e^{-\beta_4 h}}\left[\left(A_6 + A_8\right)\beta_1 e^{-\beta_1 h} + A_7\beta_2 e^{-\beta_2 h} + A_9\beta_3 e^{-\beta_3 h}\right],$$

$$A_{11} = \frac{-\left(A_4 G_r + A_1 G_c\right)}{\beta_1^2 - \beta_1 - N},$$

$$A_{12} = \frac{-A_5 G_r}{\beta_3^2 - \beta_3 - N},$$

$$A_{13} = \frac{B}{N},$$

$$A_{14} = \frac{1}{e^{-\beta_5 h}}\left[U_P - \left(A_{11} e^{-\beta_1 h} + A_{12} e^{-\beta_3 h} + A_{13}\right)\right],$$

$$A_{15} = \frac{-\left(A_6 + A_8\right)G_r - A_2 G_c + AA_{11}\beta_1}{\beta_1^2 - \beta_1 - \left(N + n\right)},$$

$$A_{16} = \frac{-A_7 G_r - A_3 G_c}{\beta_2^2 - \beta_2 - \left(N + n\right)},$$

$$A_{17} = \frac{-A_9 G_r + AA_{12}\beta_3}{\beta_3^2 - \beta_3 - \left(N + n\right)},$$

$$A_{18} = \frac{-A_{10} G_r}{\beta_4^2 - \beta_4 - \left(N + n\right)},$$

$$A_{19} = \frac{AA_{14}\beta_5}{\beta_5^2 - \beta_5 - \left(N + n\right)},$$

$$A_{20} = \frac{AA_{15}}{\beta_6^2 - \beta_6 - \left(N + n\right)},$$

$$A_{21} = \frac{1}{e^{-\beta_6 h}}\left[A_{15} e^{-\beta_1 h} + A_{16} e^{-\beta_2 h} + A_{17} e^{-\beta_3 h} + A_{18} e^{-\beta_4 h} + A_{19} e^{-\beta_5 h} + A_{20} e^{-\beta_6 h}\right].$$